British Journal of Pharmacology (2005) 145, 166–177
www.nature.com/bjp

Inhibition of TGF-β signaling by an ALK5 inhibitor protects rats from dimethylnitrosamine-induced liver fibrosis

*,[1]Anne-Charlotte de Gouville, [1]Valerie Boullay, [1]Gael Krysa, [1]Julia Pilot, [1]Jean-Marie Brusq, [1]Florence Loriolle, [1]Jean-Michel Gauthier, [2]Stephen A. Papworth, [3]Alain Laroze, [3]Françoise Gellibert & [1]Stephane Huet

[1]Biology Department, GlaxoSmithKline, 25 avenue du Quebec, Les Ulis 91951, France; [2]Pathology Department, GlaxoSmithKline, Park Road, Ware, Herts SG12 0DP and [3]Medicinal Chemistry Department, GlaxoSmithKline, 25 avenue du Quebec, 91951 Les Ulis, France

1 Chronic liver disease is characterized by an exacerbated accumulation of matrix, causing progressive fibrosis, which may lead to cirrhosis. Transforming growth factor beta (TGF-β), a well-known profibrotic cytokine, transduces its signal through the ALK5 ser/thr kinase receptor, and increases transcription of different genes including PAI-1 and collagens. The identification of GW6604 (2-phenyl-4-(3-pyridin-2-yl-1*H*-pyrazol-4-yl)pyridine), an ALK5 inhibitor, allowed us to evaluate the therapeutic potential of inhibiting TGF-β pathway in different models of liver disease.

2 A cellular assay was used to identify GW6604 as a TGF-β signaling pathway inhibitor. This ALK5 inhibitor was then tested in a model of liver hepatectomy in TGF-β-overexpressing transgenic mice, in an acute model of liver disease and in a chronic model of dimethylnitrosamine (DMN)-induced liver fibrosis.

3 *In vitro*, GW6604 inhibited autophosphorylation of ALK5 with an IC_{50} of 140 nM and in a cellular assay inhibited TGF-β-induced transcription of PAI-1 (IC_{50}: 500 nM). *In vivo*, GW6604 (40 mg kg^{-1} p.o.) increased liver regeneration in TGF-β-overexpressing mice, which had undergone partial hepatectomy. In an acute model of liver disease, GW6604 reduced by 80% the expression of collagen IA1. In a chronic model of DMN-induced fibrosis where DMN was administered for 6 weeks and GW6604 dosed for the last 3 weeks (80 mg kg^{-1} p.o., b.i.d.), mortality was prevented and DMN-induced elevations of mRNA encoding for collagen IA1, IA2, III, TIMP-1 and TGF-β were reduced by 50–75%. Inhibition of matrix genes overexpression was accompanied by reduced matrix deposition and reduction in liver function deterioration, as assessed by bilirubin and liver enzyme levels.

4 Our results suggest that inhibition of ALK5 could be an attractive new approach to treatment of liver fibrotic diseases by both preventing matrix deposition and promoting hepatocyte regeneration.
British Journal of Pharmacology (2005) **145,** 166–177. doi:10.1038/sj.bjp.0706172
Published online 21 February 2005

Keywords: Hepatectomy; collagen; ALK5; hepatic stellate cells; liver fibrosis; DMN; TGF-β; GW6604

Abbreviations: ALAT, alanine aminotransferase; ALK5, activin-like kinase 5; ASAT, aspartate aminotransferase; BMP, bone morphogenic protein; BrdU, bromodeoxyuridine; COL IA1, collagen IA1; COL IA2, collagen IA2; COL III, collagen III alpha chain; DMN, dimethylnitrosamine; DMSO, dimethylsulfoxide; DTT, dithio threitol; HSC, hepatic stellate cells; LAP, latency-associated peptide; PAI-1, plasminogen activator inhibitor-1; PCNA, proliferating cell nuclear antigen; TGF-β, transforming growth factor beta; TIMP-1, tissue inhibitor of metalloproteinase 1

Introduction

Transforming growth factor beta (TGF-β) is a pleiotropic cytokine involved in a variety of biological processes including development, cell growth, differentiation, cell adhesion, migration, extracellular matrix deposition, and the immune response (Massague *et al*., 2000). Dysregulation of TGF-β production or response has been implicated in pathologies such as atherosclerosis, cancer, and fibrosis (Blobe *et al*., 2000). The role of TGF-β as a potent profibrotic cytokine has been demonstrated in a number of animal models (Border & Noble, 1994; Kopp *et al*., 1996) and overexpression of TGF-β in transgenic mice results in liver and kidney fibrosis (Sanderson *et al*., 1995). In human, elevated TGF-β1 levels can be measured in the serum and urine of patients with hepatitis (Bayer *et al*., 1998) diabetic nephropathy as well as other fibrotic diseases (Broekelmann *et al*., 1991; Border & Noble, 1994; Shah *et al*., 1999). In liver biopsies from patients with chronic liver diseases of various aetiologies, TGF-β expression or mRNA levels are increased and correlate with the extent of fibrosis (Paradis *et al*., 1996; Kanzler *et al*., 2001).

TGF-β has direct and indirect effects on matrix accumulation; it triggers expression of collagen genes and limits matrix degradation by decreasing the expression of stromelysin and

*Author for correspondence;
E-mail: anne-charlotte.m.degouville@gsk.com
Published online 21 February 2005

increasing PAI-1 expression, thus reducing plasmin (Lund *et al*., 1987; Westerhausen *et al*., 1991; Matrisian *et al*., 1992). Following liver damage, hepatic stellate cells (HSC) differentiate into myofibroblast-like cells, which proliferate and produce matrix in response to TGF-β (Li & Friedman, 1999). Data obtained in TGF-β-overexpressing mice demonstrate that TGF-β may also directly act on parenchymal cells by inhibiting hepatocyte proliferation as observed in a liver regeneration model (Bottinger *et al*., 1996). In chronic liver disease, TGF-β may exert detrimental effects through both its action on matrix-producing cells and on hepatocytes, thus preventing organ repair and leading to progressive loss of liver function.

TGF-β1, and related members of the TGF-β superfamily, activins and bone morphogenic proteins (BMP), transduce their signal through structurally related receptors (Attisano & Wrana, 2002; Shi & Massague, 2003). Upon ligand binding to the cell surface type II receptor, heteromerization with a cell type and ligand-specific type I receptor takes place (ALK5 or ALK1 for TGF-β, ALK4 and ALK2 for activins, ALK3 or ALK6 for BMPs). Phosphorylation of a Gly-Ser-rich region of the ALK5 receptor by type II receptor activates the ALK5 ser/thr kinase catalytic domain, which subsequently phosphorylates Smad2 or Smad3 proteins (Huse *et al*., 1999). After forming a complex with a cytosolic Smad4, phosphorylated Smad2 and Smad3 translocate to the nucleus driving transcription of specific genes.

In various models of kidney or lung fibrosis, reducing TGF-β levels with angiotensin-converting enzyme inhibitors or neutralizing TGF-β activity with blocking antibodies, soluble TGF-β type II receptors or a natural TGF-β binding protein such as decorin, have been associated with beneficial antifibrotic effects (Peters *et al*., 1998; Wang *et al*., 1999; Ziyadeh *et al*., 2000; Kolb *et al*., 2001). Intravenous injection of an adenovirus expressing a dominant-negative TGF-β type II receptor showed antifibrotic effects in a rat model of dimethylnitrosamine (DMN)-induced liver fibrosis, thereby validating this model as TGF-β dependent (Nakamura *et al*., 2000). In a model of bile duct ligation-induced liver fibrosis, adenoviral expression of TGF-β antisense was proved effective in preventing liver fibrosis (Arias *et al*., 2003). Based on these observations, TGF-β signaling would appear to be a potential target for the prevention or treatment of fibrotic diseases. Therefore, direct inhibition of ALK5 represents an attractive way to prevent detrimental profibrotic effects of TGF-β. Recently described synthetic inhibitors of ALK5 have been shown to block TGF-β effects in cellular assays (Callahan *et al*., 2002; Inman *et al*., 2002; Laping *et al*., 2002; Sawyer *et al*., 2003), but their activity in animal fibrosis models is still unknown.

Here, we describe for the first time the *in vivo* activity of a new ALK5 inhibitor and show that GW6604 (2-phenyl-4-(3-pyridin-2-yl-1*H*-pyrazol-4-yl)pyridine) prevents fibrosis progression in rat models of liver fibrosis.

Methods

Chemical synthesis

GW6604 (Figure 1) was prepared as described previously (Gellibert & Mathews, 2002).

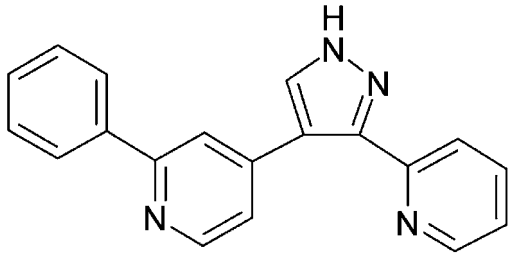

Figure 1 Structure of GW6604.

Alk5 autophosphorylation assay

The kinase domain of ALK5 (Franzen *et al*., 1993) (amino acids 162–503) was cloned by PCR and expressed in a baculovirus/Sf9 cells system. The protein was 6-His tagged in C-terminus and purified by affinity chromatography using an Ni^{2+} column. The material thus obtained was used to assess the ability of test compounds to inhibit ALK5 autophosphorylation.

Purified enzyme (10 nM) in 50 μl of Tris buffer (Tris 50 mM, pH 7.4; NaCl 100 mM; $MgCl_2$ 5 mM; $MnCl_2$ 5 mM; DTT 10 mM) was preincubated with different concentrations of compounds (0.1% dimethylsulfoxide (DMSO) final concentration in the test) for 10 min at 37°C. The reaction was initiated by the addition of 3 μM ATP (0.5 μCi gamma-^{33}P-ATP). After 15 min at 37°C, phosphorylation was stopped by the addition of SDS–PAGE sample buffer (50 mM Tris-HCl (pH 6.9), 2.5% glycerol, 1% SDS, 5% beta-mercaptoethanol). Samples were boiled for 5 min at 95°C and run on a 12% SDS–PAGE. Dried gels were exposed to a phosphor screen overnight. ALK5 autophosphorylation was quantified using a Storm imaging system (Molecular Dynamics).

Fluorescence polarization kinase binding assays

Compound binding to ALK5 was tested on purified recombinant GST-ALK5 (residues 198–503). Displacement of a rhodamine green fluorescently labeled ATP-competitive inhibitor (described in patent application WO02/24680, 2000) by different concentrations of test compounds was used to calculate a binding pIC_{50}. GST-ALK5 was added to a buffer containing 62.5 mM Hepes (pH 7.5), 1 mM DTT, 12.5 mM $MgCl_2$, 1.25 mM CHAPS (all reagents obtained from Sigma, l'Isle d'Abeau chesnes, France), and 1 nM rhodamine green-labeled ligand so that the final ALK5 concentration is 10 nM based on active site titration of the enzyme. A measure of 40 μl of the enzyme/ligand reagent was added to 384-well assay plates containing 1 μl of different concentrations of test compound. The plates are read immediately on an LJL Acquest fluorescence reader (Molecular Devices) with excitation, emission, and dichroic filters of 485, 530, and 505 nm, respectively. The fluorescence polarization for each well is calculated by the Acquest and is then imported into curve fitting software for construction of concentration–response curves. The same assay conditions were used to measure binding of GW6604 to other kinases.

Cellular assays to measure anti-TGF-β *activity of ALK5 inhibitors*

Compound activity was tested in a transcriptional assay in HepG2 cells (ATCC). Cells were stably transfected with a

reporter construct comprising the human PAI-1 promoter (−806 to +72 region) driving a luciferase (firefly) reporter gene or with a construct containing nine adjacent copies of a previously described Smad binding site (Dennler *et al*., 1998). The stably transfected cell lines were obtained by a limiting dilution method and clonal expansion of a selected clone. The cell line containing the human PAI-1 promoter (−806 to +72) responded to TGF-β stimulation with a 10- to 20-fold increase in luciferase activity compared to control conditions, whereas the cell line containing the nine adjacent Smad binding sites was highly responsive to TGF-β stimulation with a >500-fold increase in luciferase activity following the addition of TGF-β.

To test anti-TGF-β activity of a compound, cells were seeded in 96-well microplates at a concentration of 35,000 cells per well in 200 μl of serum-containing medium. Microplates were then placed for 24 h in a cell incubator at 37°C, 5% CO_2 atmosphere. Cells were then cultured in serum-free BME medium (Invitrogen, Cergy Pontoise, France) and GW6604 was added at concentrations of 10 nM to 10 μM (final concentration of DMSO 1%) 30 min prior to the addition of recombinant TGF-β1 (1 ng ml^{-1}) (R&D systems, Lille, France). After an overnight incubation, cells were washed with PBS and lysed by the addition of 10 μl of passive lysis buffer (Promega, Carbonières, France). Inhibition of luciferase activity relative to control groups was used as a measure of compound activity. A concentration–response curve was constructed from which an IC_{50} value was determined graphically.

Cellular assays for activin and BMP signaling

Compound activity *versus* activin and BMP signaling was evaluated using analogous cellular assays to that described above. Activin signaling blocking activity was tested on the HepG2 clone used for the TGF-β assay. The BMP activity assay used HepG2 cells stably transfected with a luciferase reporter driven by a BMP-responsive element (Kunasagi *et al*., 2000). Cells were preincubated with compounds for 30 min and then challenged with either activin A (50 ng ml^{-1}) or BMP6 (10 ng ml^{-1}) (R&D systems). Luciferase activity was used as readout.

Animal protocols

All experimental protocols were performed in accordance with the policies of the Institutional Animal Care and Use Committee. Animals were fed with a standard diet and had free access to water.

Acute DMN model

Acute DMN model was set up after careful study of the DMN-induced fibrosis development. The aim was to be able to detect as early as possible gene changes related to fibrogenesis and ultimately test compound activity *in vivo* in a short time frame.

Male Sprague–Dawley rats weighing 200–225 g were treated for 3 consecutive days (days 1–3) with 12.5 mg kg^{-1} i.p. DMN (Sigma), or saline. Animals were then treated twice a day with GW6604 p.o. or its vehicle (20% HCl 1 N, 80% hydroxypropyl-methylcellulose (0.5%), Tween 80 (5%), adjusted to pH 4) in a volume of 4 ml kg^{-1} on days 6, 7, and 8. Animals were killed by CO_2 inhalation on day 8, 2 h after the fifth administration of GW6604 or vehicle. Livers were collected for collagen IA1 (COL IA1) mRNA quantification by RT–PCR. Results are reported as the percent inhibition of DMN-induced increase in COL IA1 compared to control. COL IA1 mRNA was quantified

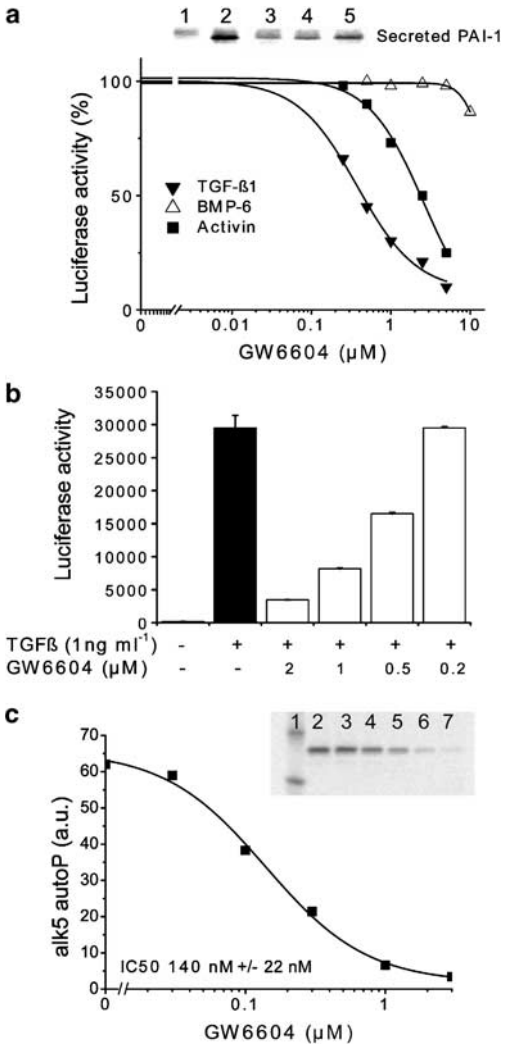

Figure 2 *In vitro* characterization of GW6604. (a) Effects of GW6604 on TGF-β, activin, and BMP6 signaling in HepG2 cell lines stably transfected with luciferase reporter genes: an HepG2 cell line containing the PAI-1 promoter (−806/+72) was used for TGFb and activin assays and a cell line containing a BMP-responsive element was used for the BMP assay (Kunasagi *et al*., 2000). Upper gel: effect of GW6604 on TGF-β-induced PAI-1 secretion: (1) control medium, (2) TGF-β (1 ng ml^{-1}), and (3–5) TGF-β in the presence of 2, 1, and 0.5 μM of GW6604. (b) Dose ranging effects of GW6604 on TGF-β-induced transcriptional activity of a Smad-responsive promoter. This stably transfected HepG2 cell line was highly responsive to TGF-β with a >500-fold increase in luciferase activity when compared to cells treated with control medium. (c) Dose ranging effect of GW6604 in the ALK5 autophosphorylation assay. In the right top is a representative SDS–PAGE autophosphorylation image of a dose range experiment with GW6604 (from three experiments giving similar results): (1) molecular weight markers, (2) ALK5 (control), and (3–7) correspond to ALK5 autophosphorylation in the presence of increasing concentrations of GW6604 (30 nM, 100 nM, 300 nM, 1 μM and 3 μM, respectively).

Table 1 Selectivity of GW6604 against a panel of kinases

	ALK5 (*)	*ALK5 binding*	*TGFβ-RII (*)*	*P38MAPK*	*VEGFR2*	*P56lck*	*ITK*	*LYN*	*Tie-2*	*Src*
GW6604 IC_{50} (μM)	0.14	0.107	10	9.5	>6	>10	>10	>10	>10	>10

Except for assays marked with (*), which refer to autophosphorylation assays, all tests were performed in a fluorescence polarization assay mode where displacement of rhodamine green-fluorescently labeled ATP-competitive inhibitor by different concentrations of GW6604 was used to calculate a binding IC_{50}. Activity of GW6604 against ALK5 was tested as described in Methods. As a control, SB203580, a reference P38MAPK inhibitor (Gallagher *et al*., 1995) was tested in the ALK5 autophosphorylation assay and showed a 3.3 μM IC_{50}. In the P38MAPK binding assay, SB203580 had a 0.06 μM binding affinity compared to 9.5 μM for GW6604.

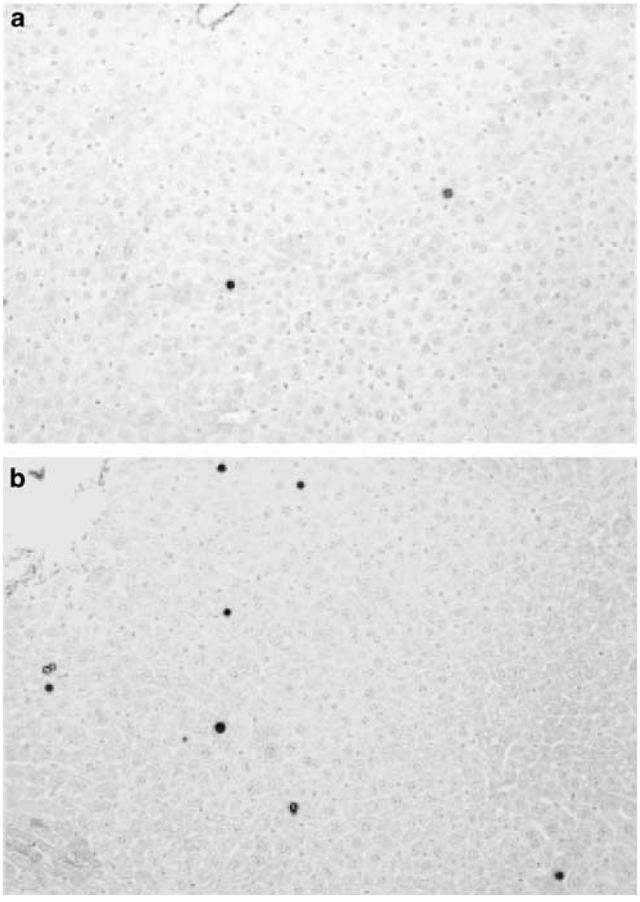

Figure 3 Effect of GW6604 (40 mg kg^{-1} p.o.) on liver regeneration in partially hepatectomized TGF-β transgenic mice. Representative photomicrograph of anti-BrdU staining of liver sections from hepatectomized animals treated with control vehicle (a) and from animals treated with GW6604 (b). Quantification of BrdU-labeled cells showed that GW6604 induced a 4.7-fold increase in the number of stained cells in transgenic animals when compared to vehicle treated animals, *versus* a nonsignificant 1.1-fold increase labeling in nontransgenic control animals ($P=0.02$, *t*-test).

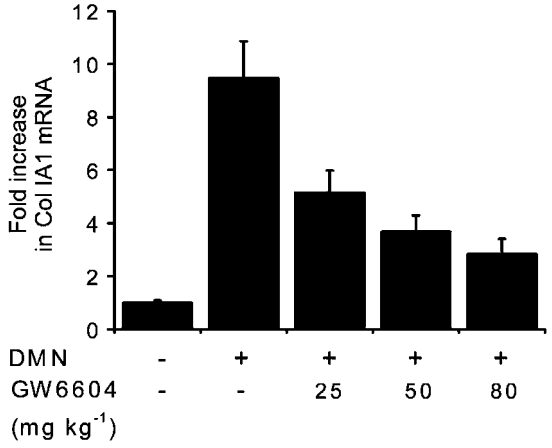

Figure 4 Effect of GW6604 on liver COL IA1 mRNA expression in the acute DMN model. Animals received a daily i.p. injection of DMN (12.5 mg kg^{-1}) for 3 consecutive days and treatment with GW6604 or vehicle given orally twice a day was initiated 72 h after the last injection of DMN. Animals were treated with GW6604 or vehicle for 3 days and COL IA1 mRNA levels were measured by quantitative RT–PCR and normalized to ribosomal 18S RNA levels as described in Methods. Difference in COL IA1 mRNA between DMN-GW6604 and DMN-vehicle was statistically significant ($P<0.05$ for the 25 mg kg^{-1} dose and $P<0.01$ for higher doses).

relative to ribosomal 18S. Four to six rats were used in each group.

Chronic DMN model

Male Sprague–Dawley rats weighing 200–225 g were treated for 6 weeks, 3 consecutive days each week with 10 mg kg^{-1} i.p. of DMN, or saline. After 3 weeks of DMN administration, treatment with GW6604 (80 mg kg^{-1} p.o., b.i.d.) or its vehicle in a volume of 4 ml kg^{-1} was initiated and continued for 3 weeks. DMN administration was continued during the 3-week treatment period. At the end of the 6-week period, animals were killed by CO_2 inhalation. Blood was collected for laboratory analysis of ALAT, ASAT, total bilirubin, alkaline phosphatase, and hyaluronic acid. Livers were collected for RT–PCR quantification of genes encoding for COL IA1, collagen IA2 (COL IA2), collagen III alpha1 chain (COL III), TIMP-1, TGF-β1, and for histologic assessment. Changes in liver messenger RNA levels relative to 18S are reported as fold induction compared to saline-vehicule, group. Mortality is reported at the end of the 6-week treatment period. All animals survived the initial 3 weeks of DMN treatment.

Partial hepatectomy and liver regeneration in TGF-β transgenic mice

Transgenic mice overexpressing TGF-β line 25 described by Sanderson *et al*. (1995) were used. Mice of similar genetic background (C57BL/6J $\times$ CBA)F1 were used as control. Partial hepatectomy (70%) was performed under gaseous anesthesia: the main portion of each hepatic lobe was isolated from the circulation by ligation, sectioned, and cauterized. Caution was taken to preserve vena cava circulation and gall bladder. After surgery, abdomen was sutured

Table 2 Effect of GW6604 in the chronic DMN model of liver fibrosis

	Saline + vehicle	*Saline + GW6604*	*DMN + vehicle*	*DMN + GW6604*
Mortality/number of rats at day 1	0/7	0/7	7/16	0/11
Liver weight (g)	15.1 ± 0.7	18.9 ± 1.8	9 ± 1.4*	17.3 ± 0.5#
18S mRNA	1.0 ± 0.01	1.01 ± 0.003	1.03 ± 0.003	1.01 ± 0.006
COL IA1 mRNA	1 ± 0.3	0.5 ± 0.08	10.9 ± 2.03*	3.7 ± 1.04#
COL IA2 mRNA	1 ± 0.25	0.5 ± 0.09	6.4 ± 0.82*	2.7 ± 0.72#
COL III mRNA	1 ± 0.13	0.7 ± 0.09	3.0 ± 0.6*	2.0 ± 0.45
TIMP-1 mRNA	1 ± 0.34	0.7 ± 0.16	14.0 ± 2.72*	4.2 ± 1.08#
TGF-β1 mRNA	1 ± 0.16	1.0 ± 0.35	6.8 ± 0.81*	2.7 ± 0.37#

mRNA encoding for COL IA1, COL IA2, COL III, TIMP-1, and TGF-β are quantified relative to 18S, which as shown above is not modified by any of the treatments.
*Statistically (t-test) significant difference between DMN + vehicle and saline + vehicule groups ($P<0.01$).
#Statistically significant difference ($P<0.01$) between DMN + GW6604 and DMN + vehicle groups.

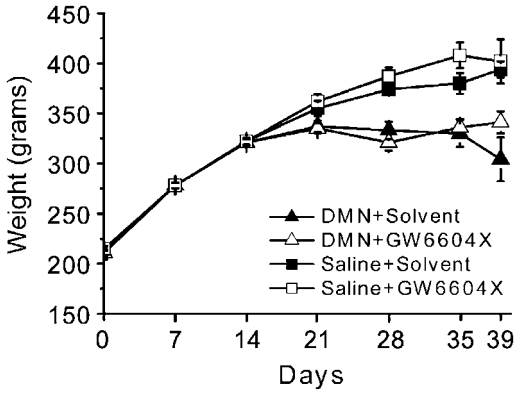

Figure 5 Weight progression curves during the 6-week chronic DMN administration study. At the end of the 6-week follow-up, differences in animal weight between saline and DMN-treated animals were statistically significant for both vehicle and GW6604-treated animals (t-test, $P<0.001$). Difference between DMN-vehicle and DMN-GW6604-treated animals was not statistically significant.

and mice kept in a warm area until complete recovery. Mice ($n=4$/group) were killed by CO_2 inhalation, 40 h after surgery, a time corresponding to a peak of mitosis. Treatment with the ALK5 inhibitor was initiated 1 h before surgery, 4 h after, and then every 12 h by oral gavage in a volume of 100 μl. Last dosing was carried out 2 h before killing. To allow quantification of cell proliferation, an i.p. administration of bromodeoxyuridine (BrdU) (0.1 mg) (Sigma) was performed 2 h before killing. BrdU incorporation was quantified by immunostaining using an anti-BrdU antibody (DAKO, Trappes, France).

Histological sample preparations for light and electron microscopy

Livers were fixed in neutral-buffered formalin, embedded in paraffin, and sections of 4 μm were prepared. Liver sections were stained with hematoxylin–eosin or Sirius red (Sweat *et al*., 1964) in order to assess liver damage and fibrosis development. Sirius red-stained sections were used to quantify fibrosis by image analysis (visilog software, Noesis, Les Ulis, France). Quantification of areas stained with Sirius red was carried out on four microscopic fields per slide and results are expressed as stained pixels/field. Immunostaining for proliferating cell nuclear antigen

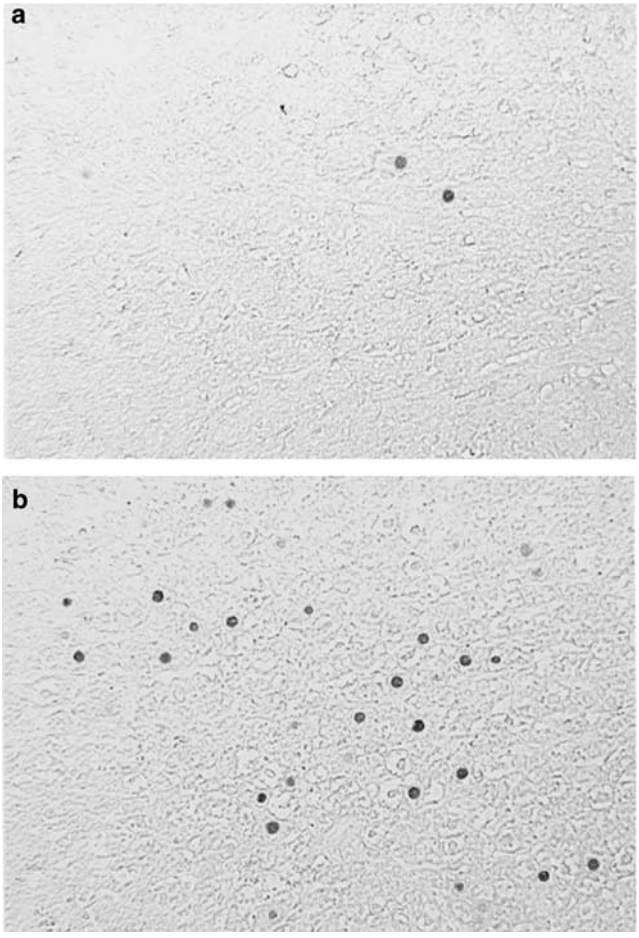

Figure 6 Immunohistochemistry for PCNA of rat liver sections. Animals received DMN for 6 weeks and were treated with vehicle (a) or GW6604 (b) from week 4 to 6 as described in Methods. In the later group, a 10-fold increase in regenerating hepatocytes was observed.

(PCNA) (DAKO) to detect proliferating cells was carried out to assess hepatic regeneration. Immunostaining for smooth muscle α-actin (Sigma) was used to detect hepatic stellate cells/myofibroblasts (Cassiman *et al*., 2002).

For electron microscopy examination, the samples were initially fixed in phosphate-buffered 4% formalde-

hyde/1% glutaraldehyde (McDowell & Trump, 1976). They were then postfixed in 1% Millonigs' buffered osmium tetroxide and processed into Spurr's resin. Toluidine blue-stained survey sections (1 μm) were prepared and examined by light microscopy to locate the areas of interest. Ultra-thin sections 60–90 nm were then prepared, stained with uranyl acetate and lead citrate, and examined in a Philips CM10 transmission electron microscope, operated at 60 kV. Examination of the sections was carried out and particular attention was paid to stellate cells phenotype and numbers. A count of these cells was carried out in the liver of one representative animal of each group. Approximatly 170 grid squares were counted for each sample.

Messenger RNA quantification by RT–PCR

Messenger RNAs were quantified by RT–PCR using an ABI prism 7700 sequence detection system (Applied Biosystem). All genes were quantified relative to 18S (Taqman ribosomal RNA control reagent, Applied Biosystem). Primer sequences for COL IA1, COL IA2, COL III, TGF-β1, and TIMP-1 are shown below:

COL IA1: ATGTTCAGCTTTGTGGACCT (forward)
CAGCTGACTTCAGGGATGT (reverse);
COL IA2: CAATGGTGGCAGCCAGTTTG (forward)
CCAGGTACGCAATGCTGTTCTT (reverse);

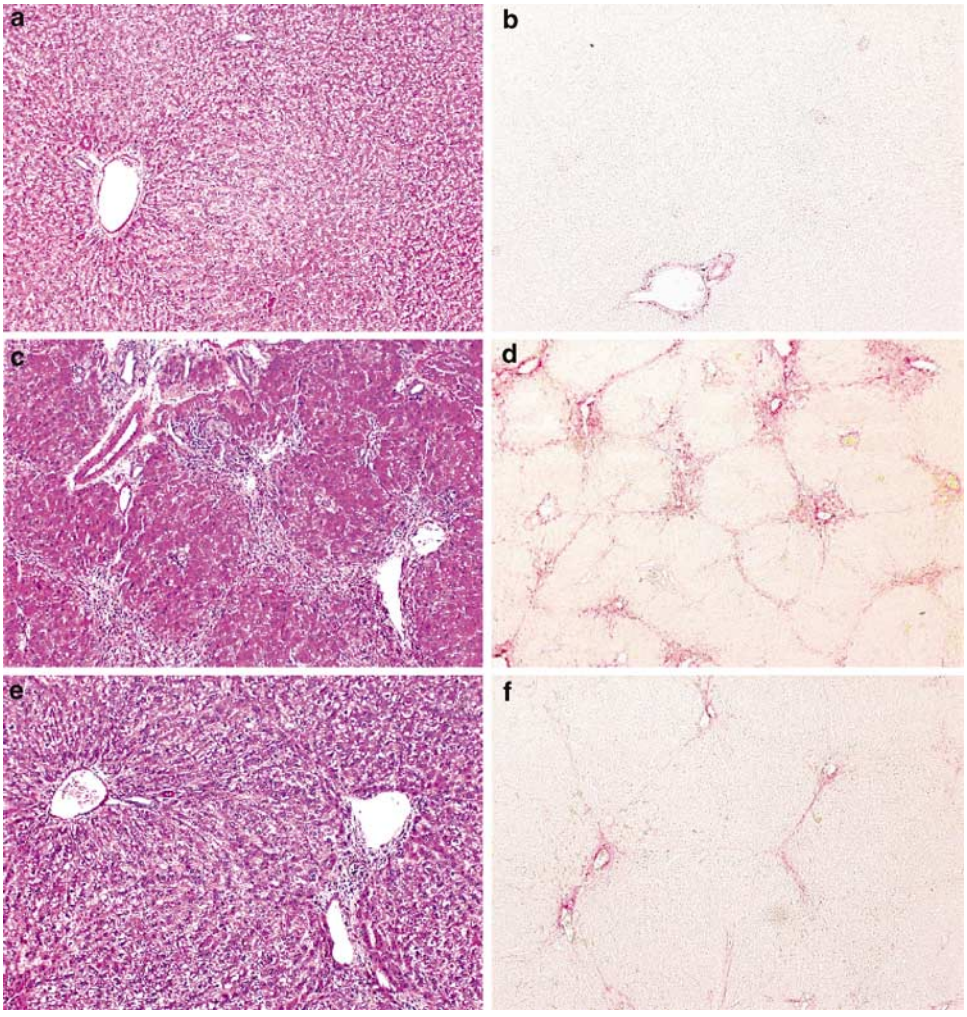

Figure 7 Liver histology. Representative photomicrograph of rat liver sections from the chronic DMN study. Hematoxylin/eosin staining (a, c, and e) and Sirius red staining (b, d, and f) of liver sections from control (a and b), DMN animals treated with vehicle (c and d), and DMN animals treated with GW6604 (e and f).

Table 3 Quantification of liver collagen content

	Saline + vehicle	*Saline + GW6604*	*DMN + vehicle*	*DMN + GW6604*
Collagen area (pixel/field)	1571 + 72	1568 + 80	34,809 + 2978*	11,229 + 1072$^{\#}$

Sirius red-stained areas were quantified by image analysis. Results are reported as stained pixel by microscopic field.
*Statistically (ANOVA test) significant difference between DMN + vehicle and saline + vehicule groups ($P<0.001$).
$^{\#}$Statistically significant difference ($P<0.001$) between DMN + GW6604 and DMN + vehicule groups.

COL III: GCCATGAGACTCCCCATCATAGATATC (forward)
CTTATAAAAAGCAAACAGGGCCAATGT (reverse);
TIMP-1: GCCTACACCCCAGCCATGGA (forward)
CGGCCCGCGATGAGAAAC (reverse);
TGF-β1: CGGACTACTACGCCAAAGAAGT (forward)
TGGTTTTGTCATAGATTGCGTT (reverse).

After collection, livers were kept at -20°C in RNAlater. RNAs were then extracted using the RNAble kit (Eurobio, France). Reverse transcription of 1 μg of total RNA was carried out using the Taqman reverse transcription reagent (Applied Biosystem). PCR was performed using the sybr-green technology in a final volume of 25 μl. Briefly, 5 μl of cDNA were mixed with 12.5 μl of sybr-green master mix and 0.1 μl of each primer (50 pmol μl^{-1}); after a 10 min incubation at 95°C, amplification was achieved by 40 cycles of 15 s at 95°C followed by 1 min at 65°C. On each amplification curve, the threshold cycle was determined and used for the quantification of mRNA using the ABI prism 7700 software.

Results

GW6604 prevents TGF-β signaling through ALK5 kinase inhibition

In HepG2 cells stably transfected with the TGF-β-responsive wild-type PAI-1 promoter driving a luciferase reporter gene, GW6604 (see structure in Figure 1) inhibited TGF-β-induced PAI-1 transcription and secretion at submicromolar concentrations ($IC_{50} = 500$ nM; Figure 2a). GW6604 selectivity *versus* activin and BMP, two members of the TGF-β superfamily, was addressed using activin- and BMP-specific cellular reporter assays. GW6604 showed a five-fold selectivity *versus* activin (IC_{50} of 2.5 μM) and did not inhibit BMP signaling ($IC_{20} > 10$ μM) (Figure 2a).

Transduction of TGF-β signaling results in Smad protein translocation to the nucleus and transcription of TGF-β-responsive genes. The Smad binding sequence in the promoter region of TGF-β-responsive genes is critical for TGF-β/Smad-induced transcription (Dennler *et al*., 1998; Shi & Massague, 2003). Using HepG2 cells transfected with an artificial reporter comprising nine adjacent copies of the Smad3/Smad4 binding sites derived from the PAI-1 promoter, we show that GW6604 inhibited the TGF-β-induced response with a potency comparable to that measured on the wild-type PAI-1 promoter, suggesting that GW6604 efficiently blocked a Smad-dependent response (Figure 2b). To further investigate the mechanism by which GW6604 inhibits TGF-β signaling, an ALK5 autophosphorylation assay was performed using a purified recombinant kinase domain. As shown in Figure 2c, GW6604 inhibited ALK5 activity with an IC_{50} of 140 nM, a potency comparable to that measured in an ALK5 binding assay ($IC_{50} = 107$ nM (Table 1). The selectivity of GW6604 for ALK5 *versus* other kinases was tested using a panel of other kinases including P38MAPK, VEGFR2, P56lck, ITK, Src, and TGF-β type II receptor; GW6604 demonstrated no significant activity on these kinases at concentrations up to 10 μM (Table 1).

GW6604 increases liver regeneration in TGF-β1-overexpressing mice

To evaluate whether GW6604 effectively blocked TGF-β effects in an *in vivo* physiological context, mice overexpressing TGF-β1 under the control of the liver-specific albumin promoter (Sanderson *et al*., 1995) were treated with GW6604 before and after partial hepatectomy and animals were killed 40 h after hepatectomy. Liver regeneration was quantified *via* BrdU labeling on five representative microscopic fields per animal. Treatment with GW6604 induced a 4.7-fold increase in

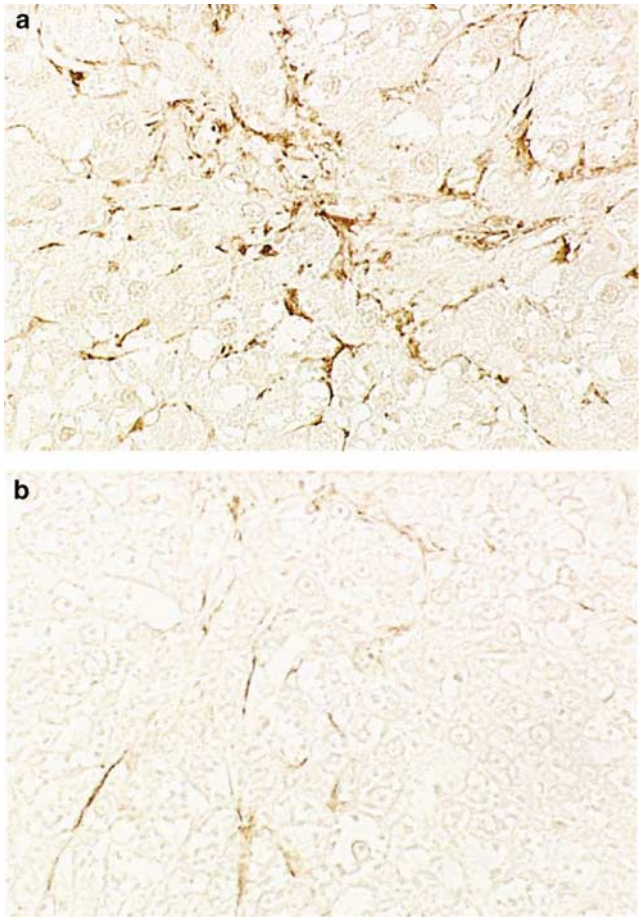

Figure 8 Immunohistochemistry for alpha smooth muscle actin in rat liver sections from the chronic DMN study. Animals received DMN for 6 weeks and were treated with vehicle (a) or GW6604 (b) from week 4 to 6 as described in Methods.

Table 4 Number and phenotype of hepatic stellate cells determined by electronic microscopy analysis of livers from vehicle and GW6604-treated animals from the chronic DMN study

	Quiescent	*Myofibroblast*	*Total*
Saline + vehicle	7.4	3.7	11.1
Saline + GW6604	7.4	3.1	10.5
DMN + vehicle	1.7	20.4	22
DMN + GW6604	4.8	3.5	9.3

Stellate cells are expressed as number per 0.1 mm^2 of liver

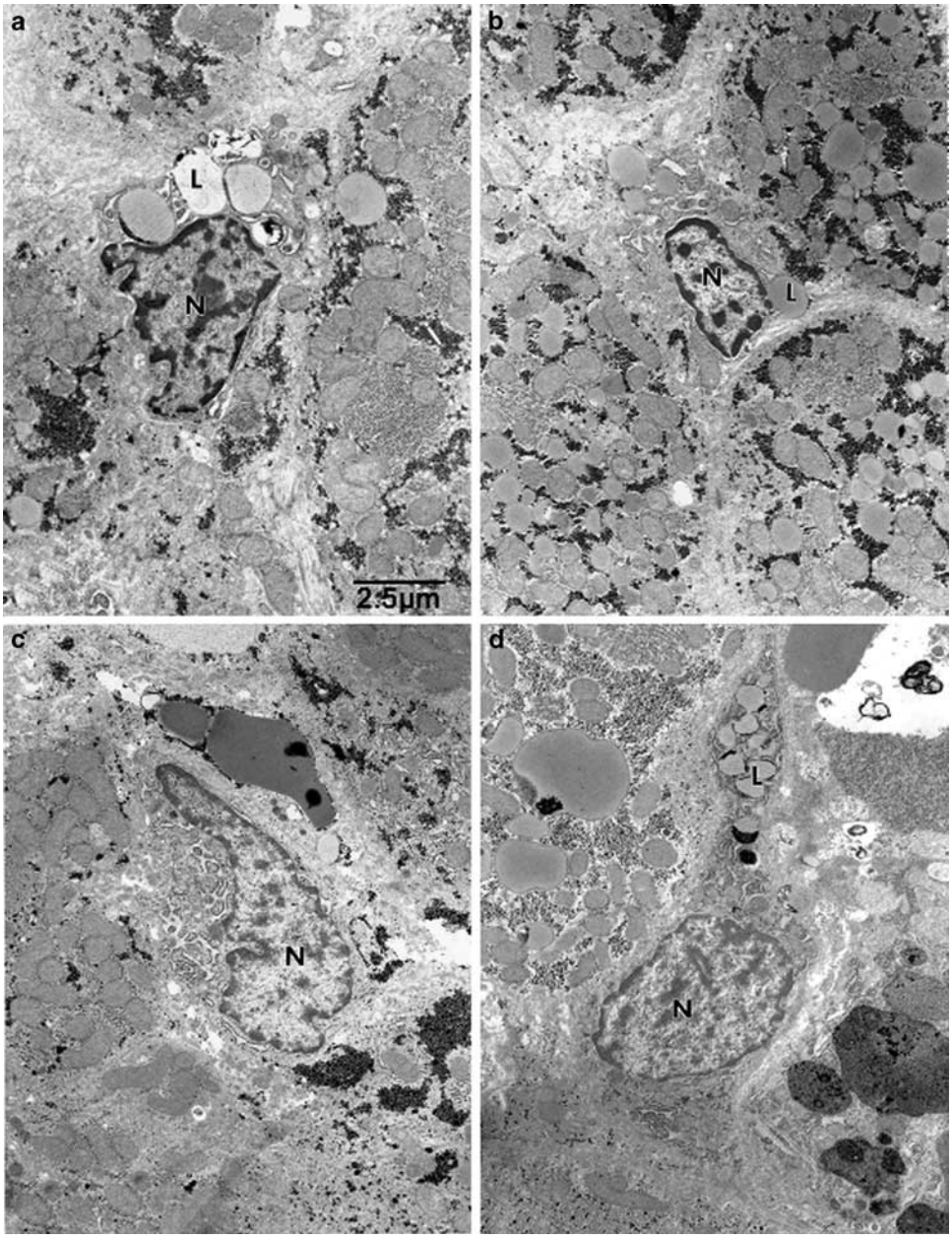

Figure 9 Representative electron microscopy images of hepatic stellate cells from a liver section obtained from (a) a control animal, (b) a control animal treated with GW6604 for 3 weeks, (c) a 6-week DMN-treated control animal and (d) a 6-week DMN-treated animal who received GW6604 (80 mg kg^{-1}, b.i.d.) for the last 3 weeks. N = nucleus of hepatic stellate cells; L = lipid droplet in hepatic stellate cell.

Table 5 Effects of GW6604 treatment on liver enzymes and hyaluronic acid in the chronic DMN model

	ASAT (IU l^{-1})	*ALAT* (IU l^{-1})	*Alkaline phosphatase* (IU l^{-1})	*Bilirubin* (mg l^{-1})	*Hyaluronic acid* (µg l^{-1})
Saline + vehicle (7)	88 ± 6	43 ± 2	225 ± 18	1 ± 0.1	107 ± 17
Saline + GW6604 (80 mg kg^{-1} twice a day) (7)	81 ± 7	47 ± 4	199 ± 22	2 ± 0.1	70 ± 11
DMN + vehicle (9)	591 ± 93**	257 ± 36**	344 ± 39*	16 ± 4**	552 ± 89**
DMN + GW6604 (80 mg kg^{-1} twice a day) (11)	126 ± 10$^{\#\#}$	82 ± 8$^{\#\#}$	249 ± 23$^{\#}$	7 ± 1$^{\#}$	222 ± 37$^{\#\#}$

(*n*) Number of animals/group at study end.
Statistically significant difference between DMN + vehicule and saline + vehicule groups ($P<0.05$, **$P<0.01$).
$^{\#}$Statistically significant difference between DMN + GW6604 and DMN + vehicule groups ($^{\#}P<0.05$, $^{\#\#}P<0.01$) (*t*-test).

hepatocyte proliferation in partially hepatectomized TGF-β transgenic animals (1.8 ± 0.4 and 8.5 ± 2.2 stained nuclei per field in animals treated with vehicle and GW6604, respectively, $P = 0.02$ (t-test)) (Figure 3). In hepatectomized nontransgenic animals and in nonhepatectomized animals treatment with GW6604 did not increase BrdU staining (data not shown). These results show that the anti-TGF-β activity of GW6604 observed *in vitro* in HepG2 cells translates into an effect on mouse hepatocytes *in vivo*.

Effect of GW6604 in an acute DMN model

During fibrogenesis, increase in COL IA1 synthesis is mainly triggered by TGF-β acting on hepatic stellate cells. In rats given DMN for 3 consecutive days, liver COL IA1 mRNA expression measured by quantitative RT–PCR was increased by about 10-fold at day 8. GW6604 (25–80 mg kg^{-1} p.o., b.i.d.) given on days 6, 7, and 8 to DMN-pretreated rats dose dependently inhibited COL IA1 overexpression (Figure 4).

Similarly, 3 days after a single administration of CCl_4 (2 ml kg^{-1} in olive oil 1 : 1) to rats, liver COL IA1 mRNA was increased by eight-fold and this increase was only 1.6-fold in rats treated with GW6604 (100 mg kg^{-1} p.o., b.i.d. for 3 consecutive days).

Therapeutic effect of GW6604 in a chronic DMN model of liver fibrosis

To demonstrate a potential therapeutic benefit of GW6604 treatment on matrix deposition and liver function, rats were given DMN for 6 consecutive weeks and received GW6604 (80 mg kg^{-1} p.o., b.i.d.) for the last 3 weeks. During the first 3 weeks of DMN administration, liver disease developed as described (Wu & Norton, 1996; George *et al*., 2001); weight progression was only slightly decreased by DMN. All rats treated with GW6604 in the DMN group (DMN-GW6604) survived the 6 weeks, whereas mortality approached 50% in the DMN-vehicle-treated group (DMN-vehicle) (Table 2). A significant decrease in liver weight was observed in the DMN-vehicle group compared to the saline-vehicle group. GW6604 prevented this decrease and maintained a normal liver weight (9 ± 1.4 g for the DMN-vehicle *versus* 17.3 ± 0.5 g for DMN-GW6604-treated animals) (Table 2). However, body weight gain was totally inhibited in both DMN-GW6604- and DMN-vehicle-treated groups (Figure 5). Immunostaining of liver section with PCNA antibodies showed very few regenerating hepatocytes in DMN-vehicle-treated rats, whereas a 10-fold increase in proliferating hepatocytes was observed in DMN-GW6604 group (Figure 6). Long-term DMN administration is known to cause chronic liver disease characterized by extensive fibrosis leading to cirrhosis (Wu & Norton, 1996; George *et al*., 2001). Analysis of liver gene expression showed that DMN treatment greatly increased mRNA encoding for matrix components (COL IA1, COL IA2, and COL III) as well as for TIMP-1 without interfering with 18S, which was used as a reference gene. In DMN-GW6604-treated animals, overexpression of mRNA encoding for TGF-β1, collagens, and TIMP-1 was reduced by 50–75% compared to DMN-vehicle group, indicating a reduction in the fibrotic process as well as an increased matrix degradation (Table 2).

Histological examination of livers showed that in rats treated for 6 weeks with DMN, liver architecture was drastically altered with necrotic areas and large fibrosis bundles linking portal spaces (Figure 7). Quantification of collagen by image analysis (Lopez-de-Leon & Rodjkind, 1985; James *et al*., 1986) showed a 22-fold increase in collagen content in the DMN-treated group and this effect was reduced to seven-fold in the group treated with GW6604 as shown in Table 3. In addition, increased numbers of myofibroblast-like cells (stained positive for smooth muscle alpha actin (α-SM)) were observed within the parenchyma (Figure 8). In the DMN-GW6604-treated rats, fibrosis was greatly reduced and the number of α-SM-positive cells was significantly decreased, although parenchyma did not completely recover a normal aspect. Electron microscopy analysis of liver sections was performed and particular attention was paid to hepatic stellate cell phenotype and number. In a quiescent phenotype, these cells store vitamin A as lipid droplets and upon liver injury differentiate into myofibroblast-like cells and lose their vitamin A content. In the control group, most stellate cells (70%) were in the quiescent state, whereas in the DMN-treated group the number of stellate cells doubled and most of them displayed a myofibroblast phenotype (90%) (Table 4). Upon treatment with GW6604 not only was the number of stellate cells similar to control groups but also most were of a vitamin A storing phenotype, indicating reduced recruitment of myofibroblasts or that GW6604-induced apoptosis of myofibroblasts (Figure 9 and Table 4). These data are consistent with the α-SM staining and the reduction in fibrosis observed in these animals.

Chronic DMN administration strongly increased ALAT, ASAT, alkaline phosphatase (PAL), and bilirubin levels. These increased levels of liver injury markers were greatly reduced in animals treated with GW6604 (Table 5) and almost normalized in the case of alkaline phosphatase. In addition, the circulating fibrosis marker hyaluronic acid (Guechot *et al*., 1994; Pontinha *et al*., 1999), which was elevated by DMN, was decreased upon treatment with GW6604, indicating again a reduction in the fibrotic process.

Discussion

Overexpression of TGF-β is a hallmark of fibrotic diseases affecting the lung, kidney, and liver. Recent reports showing the critical role played by the ALK ser/thr kinase membrane receptors and, in particular, ALK5 have stimulated interest in finding selective ALK5 inhibitors. ALK5 phosphorylates the receptor-activated Smads (R-Smads), downstream mediators of TGF-β signaling, which drive transcription of collagen genes, thereby triggering matrix deposition. This intracellular signal also induces expression of genes involved in inhibition of matrix degradation such as PAI-1 and TIMP-1. It was therefore tempting to speculate that inhibition of TGF-β signaling *via* ALK5 inhibition may have a beneficial impact on chronic fibrotic disease. To test this hypothesis, we identified inhibitors of TGF-β signaling using a cellular assay based on TGF-β-induced transcription of a luciferase reporter gene driven by the TGF-β-responsive PAI-1 promoter. This led to the identification of GW6604, which inhibited ALK5 kinase activity in an autophosphorylation assay ($IC_{50} = 140$ nM, Figure 2c). A similar affinity (IC_{50}: 107 nM) of GW6604 was also measured in a binding assay on purified recombinant ALK5 (Table 1).

GW6604 was highly selective with respect to BMP signaling and showed moderate selectivity toward activin signaling (IC_{50} TGF-β: 500 nM/activin: 2500 nM). These data are comparable with those obtained for a previously published ALK5 inhibitor (Inman *et al*., 2002; Laping *et al*., 2002), which also showed some degree of inhibition of ALK4 signaling, consistent with the high degree of homology between the ALK5 and ALK4 kinase domains (87% identity).

To demonstrate that GW6604 could effectively block TGF-β activity *in vivo*, we used a TGF-β-dependent model (transgenic mice overexpressing TGF-β in the liver) in which partial hepatectomy was performed. Bottinger *et al*. previously showed that these mice present a defect in liver regeneration due to TGF-β repressing activity on hepatocyte proliferation. In these animals, liver regeneration could be increased by injection of a TGF-β latency-associated peptide (LAP), a natural TGF-β binding protein, which prevents mature-TGF-β association and signaling through its receptor. GW6604 induced a 4.7-fold increase in hepatocyte proliferation 40 h posthepatectomy, a time corresponding to a peak of mitosis. This level is similar to that reported after LAP administration (4.5-fold increase in BrdU-stained cells) (Bottinger *et al*., 1996), demonstrating functional anti-TGF-β activity of GW6604 in a TGF-β-dependent model. Activin and BMPs transduce their signal through structurally related ALK receptors and our *in vitro* data suggest that, in addition to TGF-β signaling, activin signaling through ALK4 could also be prevented by high doses of GW6604. Follistatin, a natural activin-blocking protein has been shown to increase liver regeneration following partial hepatectomy in rodents (Phillips & De Kretser, 1998; Takabe *et al*., 2003). Based on these observations, one cannot totally exclude a contribution of activin blockade in the observed increase in hepatocyte proliferation following treatment with GW6604. However, we consider that the effect of GW6604 in this liver regeneration model is more in favor of an ALK5 *versus* ALK4 inhibitory effect for two main reasons: as mentioned above, GW6604 effects were highly comparable to those obtained following administration of the TGF-β binding protein LAP; in addition, our data obtained in partially hepatectomized nontransgenic control animals showed that GW6604 did not increase hepatocyte proliferation when compared to vehicle treated animals (a 1.1-fold nonsignificant increase).

Liver fibrosis is a complex disease involving several mediators and different cell types. Collagen overproduction, responsible for matrix accumulation in sinusoids and the portal space, is driven by myofibroblasts derived mainly from stellate cell differentiation or from other potentially fibrogenic cells with no evidence of an involvement of hepatocytes as matrix-producing cells (Weiner *et al*., 1992; Li & Friedman, 1999). Our results obtained in the liver regeneration model in TGF-β-overexpressing mice clearly demonstrated a direct effect of GW6604 on hepatocyte proliferation. Interestingly, basal expressions of COL IA1 mRNA as well as the number of matrix genes are increased in the liver and kidney of these mice when compared to control nontransgenic mice, and we observed that a 5-day treatment with GW6604 resulted in an inhibition of matrix gene expression (data not shown). To further explore the therapeutic potential of TGF-β pathway inhibition, GW6604 was tested in more complex liver fibrosis models not driven by TGF-β overexpression only. We tested GW6604 in both an acute and a chronic model of DMN-induced fibrosis. In the acute model, DMN was given to rats for 3 days and GW6604 was administered on days 6–8. This protocol was chosen to minimize a potential disease-modifying effect of GW6604 on the early phase of DMN-induced liver disease. DMN administration caused a 10-fold increase in COL IA1 mRNA expression measured by quantitative RT–PCR and this increase was dose dependently inhibited by GW6604 (Figure 4). As mentioned in the Results section, similar results were obtained in an acute CCl_4 model.

In the acute model, although an inhibitory effect on COL IA1 mRNA expression could be clearly demonstrated, histological quantification of matrix deposit to evaluate a potential benefit of GW6604 could not be performed due to the kinetics of matrix accumulation in this model (George & Chandrakasan, 2000; George *et al*., 2001). Prolonged DMN administration to rats has been shown to induce a number of pathological features observed in human chronic liver disease such as portal hypertension, cirrhosis, ascites, and biochemical abnormalities (Wu & Norton, 1996; George & Chandrakasan, 2000; Nakamura *et al*., 2000; George *et al*., 2001). The chronic experiment was set up in order to mimic a clinical situation where treatment is initiated when lesions are already advanced. In this experiment, DMN was given for 6 consecutive weeks with treatment with GW6604 starting at the beginning of the fourth week. After 3 weeks of GW6604 treatment, the most striking observation was the complete protective effect of the ALK5 inhibitor on DMN-induced mortality (no deaths in the DMN-GW6604-treated group *versus* 7/16 in the DMN-vehicle group). These results are consistent with those of Nakamura *et al*. (2000), where rats were treated with a secreted form of the TGF-β type II receptor. In our study, although all animals treated with GW6604 survived, body weight loss was not prevented by the ALK5 inhibitor, suggesting that GW6604 did not act non-specifically by preventing DMN-induced toxicity. In the DMN (vehicle) group, liver weight was decreased by almost 50% when compared to control animals, a feature of severe liver disease and fibrosis, whereas GW6604-treated animals maintained a normal or slightly increased liver size (Table 2). Immunohistological analysis of liver sections showed a 10-fold increase in PCNA staining in the DMN-GW6604 group, whereas no increase in PCNA-stained cells was observed in the control group treated with GW6604 only. Following partial hepatectomy of DMN-treated rats, Ohara also found that liver regeneration was increased by a treatment with anti-TGF-β antibodies (Ohara & Kusano, 2002). Taken together, these results are consistent with those obtained in the mouse liver regeneration model and suggest that, following liver injury in rodents, ALK5 signaling may influence and control hepatocyte proliferation. It is also possible that blocking of ALK5 signaling may prevent TGF-β-induced apoptosis (Oberhammer *et al*., 1992), and that this effect contribute to some extent to the prevention of liver weight decrease.

The beneficial antifibrotic effects of inhibiting the TGF-β pathway with GW6604 can be explained by different mechanisms. Upon treatment with GW6604, expression of collagens TIMP-1 and TGF-β genes was reduced when compared to DMN-vehicle groups. These effects could be linked to a direct effect of ALK5 inhibition on TGF-β-induced expression of matrix genes by HSC, and can also be explained by a reduction in HSC proliferation/differentiation as demonstrated by immunostaining of α-SM-positive cells and electron micro-

scopy analysis showing a reduced number of activated HSC. In an activated state, HSC secrete not only matrix components such as collagens but also TIMP-1, which inhibits matrix degradation. In addition, secreted TIMP-1 has been shown to inhibit stellate cell apoptosis *via* inhibition of matrix metalloproteases (Murphy *et al*., 2002), suggesting that the lower number of activated HSC might be due to an increased apoptosis. Reduced expression of PAI-1 mRNA in the liver was also observed in rats upon TGF-β inhibition with GW6604 (data not shown), an effect presumably translating into a decrease in PAI-1 protein, causing indirect increase in matrix degradation through increased plasmin activity as suggested by previous studies (Eitzman *et al*., 1996; Zhang *et al*., 1999). In addition, the observed reduction in TGF-β1 mRNA also suggests that ALK5 inhibition may induce a break in the TGF-β overproduction/fibrogenesis process, thus contributing to the therapeutic benefit. All of these effects of GW6604 on matrix production and liver regeneration led to an overall improvement of liver state as assessed by liver enzyme data (a reduction in ALAT, ASAT, and alkaline phosphatase). Consistent with the results of Nakamura *et al*. (2000), bilirubin levels were also significantly reduced upon ALK5 inhibition. However, it is possible that the effect on liver enzymes (ALAT and ASAT) is indirect or dependent on the fibrosis model used as in a model of bile duct ligation Arias *et al*. (2003), using TGF-β antisense mRNA, showed a decrease in matrix deposit but no normalization of liver enzymes.

In conclusion, although liver fibrosis is a multicomponent disease, TGF-β appears to play a major role as underlined by the results obtained with GW6604, a novel ALK5 inhibitor. GW6604 inhibits TGF-β signaling *in vitro* and blocks TGF-β effects *in vivo* as evidenced by its ability to increase hepatocyte proliferation following liver injury or partial hepatectomy, and also to reduce matrix gene expression in acute and chronic models of liver fibrosis. In a chronic model of DMN-induced fibrosis, GW6604 was a valuable therapeutic tool as it reduced mortality and decreased fibrosis, leading to an overall amelioration in liver function. These data suggest that blocking TGF-β effect through ALK5 inhibition represents a promising approach for the treatment of chronic liver diseases.

We thank Dr Michel Vidaud for his valuable help in designing RNA probes for quantitative PCR studies, Dr Pierre Bedossa for his precious advice on histological studies, Dr Andrew Brewster, Dr Jorge Kirilovsky, and Dr Francois Hyafil for helpful discussion, and our colleagues from the GlaxoSmithKline Kinase screening group for their technical support.

References

ARIAS, M., SAUER-LEHNEN, S., TREPTAU, J., JANOSCHEK, N., THEUERKAUF, I., BUETTNER, R., GRESSNER, A. & WEISKIRCHEN, R. (2003). Adenoviral expression of a transforming growth factor-β1 antisense mRNA is effective in preventing liver fibrosis in bile-duct ligated rats. *BMC Gastroenterol.,* **3,** 29–41.

ATTISANO, L. & WRANA, J.L. (2002). Signal transduction by the TGF-beta superfamily. *Science,* **296,** 1646–1647.

BAYER, E.M., HERR, W., KANZLER, S., WALDMANN, C., MEYER ZUM BUSCHENFELDE, K.H., DIESNE, H.P. & LOHSE, A.W. (1998). Transforming growth factor β1 in autoimmune hepatitis: correlation of liver tissue expression and serum levels with disease activity. *J. Hepatol.,* **28,** 803–811.

BLOBE, G.C., SCHIEMANN, W.P. & LODISH, H.F. (2000). Role of transforming growth factor beta in human disease. *N. Engl. J. Med.,* **342,** 1350–1358.

BORDER, W.A. & NOBLE, N.A. (1994). Transforming growth factor β in tissue fibrosis. *N. Engl. J. Med.,* **331,** 1286–1292.

BOTTINGER, E.P., FACTOR, V.M., TSANG, M.L., WEATHERBEE, J.A., KOPP, J.B., QIAN, S.W., WAKEFIELD, L.M., ROBERTS, A.B., THORGEIRSSON, S.S. & SPORN, M.B. (1996). The recombinant proregion of transforming growth factor beta1 (latency-associated peptide) inhibits active transforming growth factor beta1 in transgenic mice. *Proc. Natl. Acad. Sci. U.S.A.,* **93,** 5877–5882.

BROEKELMANN, T.J., LIMPER, A.H., COLBY, T.V. & MCDONALD, J.A. (1991). Transforming growth factor β1 is present at sites of extracellular matrix gene expression in human pulmonary fibrosis. *Proc. Natl. Acad. Sci. U.S.A.,* **88,** 6642–6646.

CALLAHAN, J.F., BURGESS, J.L., FORNWALD, J.A., GASTER, L.M., HARLING, J.D., HARRINGTON, F.P., HEER, J., KWON, C., LEHR, R., MATHUR, A., OLSON, B.A., WEINSTOCK, J. & LAPING, N.J. (2002). Identification of novel inhibitors of the transforming growth factor β 1 (TGF-β 1) type 1 receptor (ALK5). *J. Med. Chem.,* **45,** 999–1001.

CASSIMAN, D., LIBBRECHT, L., DESMET, V., DENEF, C. & ROSKAMS, T. (2002). Hepatic stellate cell/myofibroblast subpopulations in fibrotic human and rat livers. *J. Hepatol.,* **36,** 200–209.

DENNLER, S., ITOH, S., VIVIEN, D., TEN DIJKE, P., HUET, S. & GAUTHIER, J.M. (1998). Direct binding of Smad3 and Smad4 to critical TGF-B inducible elements in the promoter of human plasminogen activator inhibitor-type1 gene. *EMBO J.,* **17,** 3091–3100.

EITZMAN, D.T., MCCOY, R.D., ZHENG, X., FAY, W.P., SHEN, T., GINSBURG, D. & SIMON, R.H. (1996). Bleomycin-induced pulmonary fibrosis in transgenic mice that either lack or overexpress the murine plasminogen activator inhibitor-1 gene. *J. Clin. Invest.,* **97,** 232–237.

FRANZEN, P., TEN DIJKE, P., ICHIJO, H., YAMASHITA, H., SCHULZ, P., HELDIN, C.H. & MIYAZONO, K. (1993). Cloning of a TGF beta type I receptor that forms a heteromeric complex with the TGF beta type II receptor. *Cell,* **75,** 681–692.

GALLAGHER, T.F., FIER-THOMPSON, S.M., GARIGIPATI, R.S., SORENSON, M.E., SMIETANA, J.M., LEE, D., BENDER, P.E., LEE, J.C., LAYDON, J.T., GRISWOLD, D.E., CHABOT-FLETCHER, M.C., BRETON, J.J. & ADAMS, J.L. (1995). 2,4,5-Triarylimidazole inhibitors of IL-1 biosynthesis. *Bioorg. Med. Chem. Lett.,* **5,** 1171–1176.

GELLIBERT, F.J. & MATHEWS, N. (2002). *PCT Int. Appl.,* WO 0266462.

GEORGE, J. & CHANDRAKASAN, G. (2000). Biochemical abnormalities during the progression of hepatic fibrosis induced by dimethylnitrosamine. *Clin. Biochem.,* **33,** 563–570.

GEORGE, J., RAMESH RAO, K., STERN, R. & CHANDRAKASAN, G. (2001). Dimethylnitrosamine-induced liver injury in rats: the early deposition of collagen. *Toxicology,* **156,** 129–138.

GUECHOT, J., POUPON, R.E., GIRAL, P., BALKAU, B., GIBOUDEAU, J. & POUPON, R. (1994). Relationship between procollagen III aminoterminal propeptide and hyaluronan serum levels and histological fibrosis in primary biliary cirrhosis and chronic viral hepatitis C. *J. Hepatol.,* **20,** 388–393.

HUSE, M., CHEN, Y.G., MASSAGUE, J. & KURIYAN, J. (1999). Crystal structure of the cytoplasmic domain of the type I TGFβ receptor in complex with FKBP12. *Cell,* **96,** 425–436.

INMAN, G., NICOLAS, F., CALLAHAN, J., HARLING, J., GASTER, L., REITH, A., LAPING, N. & HILL, C. (2002). SB-431542 is a potent and specific inhibitor of transforming growth factyor-B superfamily type I activin receptor like kinase (alk) receptor ALK4, ALK5 and ALK7. *Mol. Pharmacol.,* **62,** 65–74.

JAMES, J., BOSH, K.S., ZUYDERHOUDT, F.M.J., HOUTKOOPER, J.M. & VANGOOL, J. (1986). Histomorphometric estimation of volume density of collagen as an indication of fibrosis in rat liver. *Histochemistry,* **85,** 129–133.

KANZLER, S., BAUMANN, M., SCHIRMACHER, P., DRIES, V., BAYER, E., GERKEN, G., DIENES, H.P. & LOHSE, A.W. (2001). Prediction of progressive liver fibrosis in hepatitis C infection by serum and tissue levels of transforming growth factor-beta. *J. Viral Hepatitis,* **8,** 430–437.

KOLB, M., MARGETTS, P.J., GALT, T., SIME, P.J., XING, Z., SCHMIDT, M. & GAULDIE, J. (2001). Transient gene expression of decorin in the lung reduces the fibrotic response to bleomycin. *Am. J. Respir. Crit. Care Med.,* **163,** 770–777.

KOPP, J.B., FACTOR, V., MOZES, M., NAGY, P., SANDERSON, N., BOTTINGER, E.P., KLOTMAN, P. & THORGEIRSSON, S. (1996). Transgenic mice with increased plasma levels of TGF-β1 develop progressive renal disease. *Lab. Invest.,* **74,** 991–1003.

KUNASAGI, K., INOUE, H., ISHIDOU, Y., MISHIMA, H.K., KAWABATA, M. & MIYAZONO, K. (2000). Characterisation of a bone morphogenic protein-responsive Smad-binding element. *Mol. Cell. Biol.,* **11,** 555–565.

LAPING, N., GRYGIELKO, E., MATHUR, A., BUTTER, S., BOMBERGER, J., TWEED, C., MARTIN, W., FORNWALD, J., LEHR, R., HARLING, J., GASTER, L., CALLAHAN, J.F. & OLSON, B.A. (2002). Inhibition of transforming growth factor (TGF)-b1-induced extracellular matrix with a novel inhibitor of the TGF-B type 1 receptor kinase activity: SB-431542. *Mol. Pharmacol.,* **62,** 58–64.

LI, D. & FRIEDMAN, S.L. (1999). Liver fibrogenesis and the role of hepatic stellate cells: new insights and prospects for therapy. *J. Gastroenterol. Hepatol.,* **14,** 618–633.

LOPEZ-DE-LEON, A. & RODJKIND, M. (1985). A simple micro-method for collagen and total protein determination in formalin-fixed parrafin embedded sections. *J. Histochem. Cytochem.,* **33,** 737–743.

LUND, L.R., RICCIO, A., ANDREASEN, P.A., NIELSEN, L.S., KRISTENSEN, P., LAIHO, M., SAKSELA, O., BLASI, F. & DANO, K. (1987). Transforming growth factor-beta is a strong and fast acting positive regulator of the level of type-1 plasminogen activator inhibitor mRNA in WI-38 human lung fibroblasts. *EMBO J.,* **6,** 1281–1286.

MASSAGUE, J., BLAIN, S.A. & LO, R.S. (2000). TGFβ signaling in growth control, cancer, and heritable disorders. *Cell,* **103,** 295–309.

MATRISIAN, L.M., GANSER, G.L., KERR, L.D., PELTON, R.W. & WOOD, L.D. (1992). Negative regulation of gene expression by TGF-beta. *Mol. Reprod. Dev.,* **32,** 111–120.

MCDOWELL, E.M. & TRUMP, B.F. (1976). Histological fixatives suitable for diagnostic light and electron microscopy. *Arch. Pathol. Lab. Med.,* **100,** 405–414.

MURPHY, F.R., ISSA, R., ZHOU, X., RATNARAJAH, S., NAGASE, H., ARTHUR, M.J., BENYON, C. & IREDALE, J.P. (2002). Inhibition of apoptosis of activated hepatic stellate cells by tissue inhibitor of metalloproteinase-1 is mediated *via* effects on matrix metalloproteinase inhibition: implication for reversibility of liver fibrosis. *J. Biol. Chem.,* **277,** 11069–11076.

NAKAMURA, T., SAKATA, R., UENO, T., SATA, M. & UENO, H. (2000). Inhibition of transforming growth factor beta prevents progression of liver fibrosis and enhances hepatocyte regeneration in dimethylnitrosamine-treated rats. *Hepatology,* **32,** 247–255.

OBERHAMMER, F.A., PAVELKA, M., SHARMA, S., TIEFENBACHER, R., PURCHIO, A.F., BURSCH, W. & SCHULTE-HERMANN, R. (1992). Induction of apoptosis in cultured hepatocytes and in regressing liver by transforming growth factor beta 1. *Proc. Natl. Acad. Sci. U.S.A.,* **89,** 5408–5412.

OHARA, K. & KUSANO, M. (2002). Anti-transforming growth factor-beta1 antibody improves survival rate following partial hepatectomy in cirrhotic rats. *Hepatol. Res.,* **24,** 174–183.

PARADIS, V., MATHURIN, P., LAURENT, A., CHARLOTTE, F., VIDAUD, M., POYNARD, T., HOANG, C., OPOLON, P. & BEDOSSA, P. (1996). Histological features predictive of liver fibrosis in chronic hepatitis C infection. *J. Clin. Pathol.,* **49,** 998–1004.

PETERS, H., BORDER, W.A. & NOBLE, N.A. (1998). Targeting TGF-beta overexpression in renal disease: maximizing the antifibrotic action of angiotensin II blockade. *Kidney Int.,* **54,** 1570–1580.

PHILLIPS, D.J. & DE KRETSER, D.M. (1998). Follistatin: a multi-functional regulatory protein. *Front. Neuroendocrinol.,* **19,** 287–322.

PONTINHA, N., PESSEGUEIRO, H. & BARROS, H. (1999). Serum hyaluronan as a marker of liver fibrosis in asymptomatic chronic viral hepatitis C. *Scand. J. Clin. Lab. Invest.,* **59,** 343–347.

SANDERSON, N., FACTOR, V., NAGY, P., KOPP, J., KONDAIAH, P., WAKEFIELD, L., ROBERTS, A., SPORN, M. & THORGEIRSSON, S. (1995). Hepatic expression of mature transforming growth factor β1 in transgenic mice results in multiple tissue lesions. *Proc. Natl. Acad. Sci. U.S.A.,* **92,** 2572–2576.

SAWYER, J.S., ANDERSON, B.D., BEIGHT, D.W., CAMPBELL, R.M., JONES, M.L., HERRON, D.K., LAMPE, J.W., MCCOWAN, J.R., MCMILLEN, W.T., MORT, N., PARSONS, S., SMITH, E.C.R., VIETH, M., WEIR, L.C., YAN, L., ZHANG, F. & YINGLING, J.M. (2003). Synthesis and activity of new aryl- and heteroaryl-substituted pyrazole inhibitors of the transforming growth factor-type I receptor kinase domain. *J. Med. Chem.,* **46,** 3953–3956.

SHAH, M., REVIS, D., HERRICK, S., BAILLIE, R., THORGEIRSON, S., FERGUSON, M. & ROBERTS, A. (1999). Role of elevated plasma TGF-beta1 levels in wound healing. *Am. J. Pathol.,* **154,** 1115–1124.

SHI, Y. & MASSAGUE, J. (2003). Mechanisms of TGF-beta signaling from cell membrane to the nucleus. *Cell,* **113,** 685–700.

SWEAT, F., PUCHTLER, H. & ROSENTHAL, S. (1964). Sirius red F3BA as a stain for connective tissue. *Arch. Pathol.,* **78,** 69–72.

TAKABE, K., WANG, L., LEAL, A.M., MACCONELL, L.A., WIATER, E., TOMIYA, T., OHNO, A., VERMA, I.M. & VALE, W. (2003). Adenovirus-mediated overexpression of follistatin enlarges intact liver of adult rats. *Hepatology,* **38,** 1107–1115.

WANG, Q., WANG, Y., HYDE, D.M., GOTWALS, P.J., KOTELIANSKY, V.E., RYAN, S.T. & GIRI, S.N. (1999). reduction of bleomycin induced lung fibrosis by transforming growth factor beta soluble receptor in hamsters. *Thorax,* **54,** 805–812.

WEINER, F.R., SHAH, A., BIEMPICA, L., ZERN, M.A. & CZAJA, M.J. (1992). The effects of hepatic fibrosis on Ito cell gene expression. *Matrix,* **12,** 36–43.

WESTERHAUSEN Jr, D.R., HOPKINS, W.E. & BILLADELLO, J.J. (1991). Multiple transforming growth factor-beta-inducible elements regulate expression of the plasminogen activator inhibitor type-1 gene in Hep G2 cells. *J. Biol. Chem.,* **266,** 1092–1100.

WU, J. & NORTON, P. (1996). Animal models of liver fibrosis. *Scand. J. Gastroenterol.,* **31,** 1137–1143.

ZHANG, L.P., TAKAHARA, T., YATA, Y., FURUI, K., JIN, B., KAWADA, N. & WATANABE, A. (1999). Increased expression of plasminogen activator and plasminogen activator inhibitor during liver fibrogenesis of rats: role of stellate cells. *J. Hepatol.,* **31,** 703–711.

ZIYADEH, F., HOFFMAN, B., HAN, D.C., IGLESIAS-DE LA CRUZ, M., CRUZ, M., HONG, S.W., ISONO, M., CHEN, S., MCGOWAN, T. & SHARMA, K. (2000). Long term prevention of renal insufficiency, excess matrix gene expression, and glomerular mesangial matrix expansion by treatment with monoclonal antitransforming growth factor -β antibody in db/db diabetic mice. *Proc. Natl. Acad. Sci. U.S.A.,* **97,** 8015–8020.

(Received July 27, 2004
Revised October 21, 2004
Accepted January 12, 2005)